Desalination and Water Treatment
www.deswater.com
doi: 10.1080/19443994.2014.941012

54 (2015) 1150–1157
April

Taylor & Francis
Taylor & Francis Group

The hydrodynamics of an ozone contactor with horizontal meandering flow to enhance disinfection efficiency

Dooil Kim[a], Kyung-Hyuk Lee[b], Hosun Lee[c], Yunjung Kim[d], Inhwan Hyun[a,*]

[a]*Civil and Environmental Engineering, Dankook University, Yongin, Gyeonggi-do 406-772, Korea, email: ihhyun@dankook.ac.kr (I. Hyun)*
[b]*Water and Wastewater Research Center, Korea Institute of Water and Environment, Jeonmin-dong, Yuseong, Daejeon 305-730, Korea*
[c]*Civil and Environmental Engineering, Incheon National University, Incheon 406-772, Korea*
[d]*Water Environmental Research Group, Posco E&C, Incheon 406-772, Korea*

Received 16 January 2014; Accepted 16 June 2014

ABSTRACT

The axial dispersion of an ozone contactor is known to influence *Cryptosporidium parvum* oocyst inactivation and bromate formation. While low dispersion is beneficial, an extent of dispersion is not specifically addressed for the design of a new ozone contactor. *C. parvum* oocyst inactivation, residual ozone, CT (i.e. Concentration × Time), and bromate formation were numerically simulated with diverse dispersion number (*d*), ranging from 0.01 to 5, using axial dispersion reactor model and kinetic parameters obtained from sand-filtered raw water under three pH and three temperature values. *C. parvum* oocyst inactivation was affected sensitively by the axial dispersion number especially at the region lower than 0.5. On the contrary, residual ozone, CT, and bromate formation were slightly influenced by dispersion number. The axial dispersion number of the full-scale ozone reactor with meandering horizontal flow was obtained with a tracer test. The equation for predicting the dispersion number of an ozone contactor with horizontal meandering flow was developed in the manuscript. The experimental axial dispersion number was slightly higher than the theoretically derived one because of flow disturbance in the channel of the ozone contactor.

Keywords: Ozone contactor hydrodynamics; Axial dispersion reactor model; Dispersion number; Bromate formation; Ozone disinfection

1. Introduction

Ozone disinfection has been used for drinking water treatment for more than 100 years and has proven to be effective since the strong oxidation potential of ozone is more efficient at inactivating the *Cryptosporidium parvum* oocyst than chlorine-based disinfectants [1–3]. Ozone produces much less trihalomethanes and haloacetic acids compared to free chlorine [4–6]. Encysted parasites such as *C. parvum* are more resistant to conventional chlorination and reported to cause acute water-borne diseases [7]. As ozone can effectively inactivate these encysted pathogens, the ozone reactor has been extensively adopted in the world. Ozonation

*Corresponding author.

Presented at the 6th International Conference on the "Challenges in Environmental Science and Engineering" (CESE-2013), 29 October–2 November 2013, Daegu, Korea

produces bromate, which is a by-product of the ozone disinfection process with raw water that contains natural bromide. Bromate has been classified as a potentially carcinogenic inorganic compound (category 2B) by the international agency for research on cancer [8] and limited to 10 μg/L, the maximum contamination level accepted in the United States [9]. It has been reported to be a cause of kidney cancer in laboratory animals [10].

The most ideal reactor types, frequently found in an ozone reactor design, are the continuously stirred tank reactor (CSTR) and the plug flow reactor (PFR). While the CSTR is well mixed and has uniform concentration, the PFR is characterized by plug flow that does not allow mixing between adjacent flow elements [11]. These ideal flow patterns cannot represent real flow patterns in a full-scale ozone reactor because it has short-circuiting, back-flow, and a stagnant zone. These non-ideal flow patterns increase the axial dispersion number, which is represented in Eq. (1).

$$d = \frac{E}{UL} \tag{1}$$

where E is the axial diffusivity (m^2/s), U is the axial flow velocity (m/s), and L is the axial characteristic length (m).

The axial dispersion number of an ozone reactor has crucial influence on the inactivation efficiency of *C. parvum* oocysts [12]. The importance of axial dispersion becomes more apparent when bromate formation is of concern [13–15]. Consequently, reactor hydrodynamics needs to be enhanced to minimize bromate formation while achieving the target inactivation efficiency for *C. parvum* oocysts [15,16]. The ozone contactor model (OCM) software was developed to comply with the needs and proved to be very effective in optimizing an ozone reactor design and performance targeting *C. parvum* oocyst inactivation and bromate reduction [15]. While the lower dispersion is known to be beneficial on the *C. parvum* oocyst inactivation and bromate reduction, an appropriate extent of axial dispersion number in an ozone reactor design has not been clearly addressed.

The one-dimensional axial dispersion model (ADR) has been used to represent the flow motion close to the PFR, expressed by dispersion, advection, and reaction terms. The major advantages of the ADR model over two- and three-dimensional computational fluid dynamics model are simplicity and usefulness in predicting Concentration × Time (CT), pathogen inactivation, and bromate formation [15]. Dissolved ozone, fast ozone demand, *C. parvum* oocyst, and bromate are expressed by Eqs. (2)–(5). The programming code was modified from the OCM software [15] to incorporate ozone injection using side-stream venturi injector (SVI), contrary to the fine bubble diffuser used in the OCM software.

Dissolved ozone:

$$E \cdot \frac{d^2[O_3]}{dx^2} - U\frac{d[O_3]}{dx} - k_d \cdot [O_3] - k_R \cdot [D] \cdot [O_3] = 0 \tag{2}$$

Fast ozone demand:

$$E \cdot \frac{d^2[D]}{dx^2} - U\frac{d[D]}{dx} - k_R \cdot [D] \cdot [O_3] = 0 \tag{3}$$

C. parvum oocyst:

$$E \cdot \frac{d^2N}{dx^2} - U\frac{dN}{dx} - k_N \cdot N \cdot [O_3] = 0 \tag{4}$$

Bromate:

$$E \cdot \frac{d^2[BrO_3^-]}{dx^2} - U\frac{d[BrO_3^-]}{dx} - k_{BrO3^-}[O_3] = 0 \tag{5}$$

where $[O_3]$ is dissolved ozone concentration, $[D]$ is ozone demand concentration, N is the number of *C. parvum* oocyst, $[BrO_3^-]$ is bromate concentration, E is axial dispersion coefficient, x is the distance from the inlet in the axial direction, k_D is first-order ozone decay rate constant, k_R is second-order rate constant for ozone reaction with ozone demand, $k_BrO_{3^-}$ is first-order bromate formation rate constant, and U is axial velocity. In this study, a pseudo-first-order Chick–Watson expression without an initial lag phase with a second-order inactivation rate constant, k_N in Eq. (6), was used to represent the inactivation kinetics of *C. parvum* oocysts with ozone [9].

$$k_N = 0.0917 \times 1.097^T \tag{6}$$

where T is the temperature (°C).

The objectives of this research were to investigate an extent of axial dispersion appropriate for *C. parvum* oocyst inactivation, residual ozone concentration, CT (ozone concentration times contacting time), and bromate formation using axial dispersion reactor (ADR) model and kinetic parameters obtained from influent raw water. Additionally, a method to predict the axial dispersion number of a full-scale ozone contactor with a horizontal meandering flow was developed.

2. Materials and methods

2.1. The full-scale ozone contactor

The full-scale ozone contactor is located in South Korea and has two trains each of which could treat 210,000 m^3/d of water as design capacity. The schematic diagram and dimensions of the contactor are shown at Fig. 1. The design hydraulic residence time is 15.4 min. Ozone dosing ranges from 0.5 to 2.0 mg/L. Ozone is injected using side-stream injectors and dissolved in the dissolution pipe of 9.0 m in length and 0.65 m in internal diameter. The sand-filtered water sample was obtained from a water treatment plant in South Korea. The process of water treatment is composed of coagulation/flocculation, sedimentation, sand filtration, and ozonation in series. The axial dispersion number of the full-scale ozone reactor was analyzed with a tracer test using chemically conservative Sodium Fluoride (NaF). The flow rate during the tracer test was 158,400 m^3/d.

2.2. Ozone decay and bromate formation kinetics

Ozone decay kinetic parameters were obtained from batch experiments using a multi-channel stopped_flow reactor (MC-SFR) system shown in Fig. 2 [17]. The MC-SFR system can measure ozone decay kinetics and can be used as a batch ozonation reactor for bromate formation kinetics. The details of the MC-SFR setup and experimental procedures have previously been described by Kim et al. [17]. Briefly, the MC-SFR system is composed of six tubular reactors with different reaction times. The flow can be isolated during reaction by closing solenoid valves at both sides of the tubular reactors. Reacted ozone solution flows through a UV/VIS spectrophotometer after being mixed with indigo reagent. To analyze the bromate concentration, 2–3 mL samples were collected from the outlet of the MC-SFR system and instantaneously mixed with 0.1 mL of 0.5 M ethylenediamine (EDA) solution to quench the residual ozone in a vial. The bromate and bromide ion concentrations were measured according to EPA method 317.0 using a Dionex DX-600 ion chromatography system (Dionex, Sunnyvale, CA).

3. Results and discussion

While ozone decay is affected by a diverse range of constituents in natural waters, its decay kinetics are well expressed by the first-order kinetic expression, as shown in Eq. (7) [18].

$$\frac{d[O_3]}{dt} = -k_D[O_3] \tag{7}$$

where $[O_3]$ is the liquid phase ozone concentration, t is the time, and k_D is the first-order ozone decay kinetic constant. Lev and Regli [19] incorporated a second-order rate term for natural organic matter, and changed Eq. (7) into Eqs. (8) and (9).

$$\frac{d[O_3]}{dt} = -k_D[O_3] - k_R[D]\cdot[O_3] \tag{8}$$

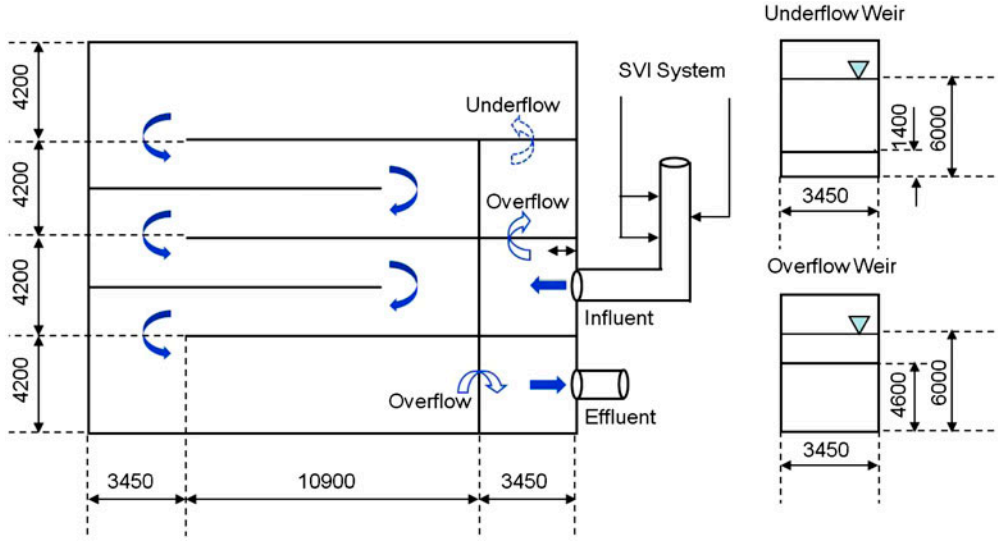

Fig. 1. Dimension and shape of one train of the full-scale ozone reactor with side-SVI system. The depth of the contactor is designed to be 6,000 mm (unit: mm).

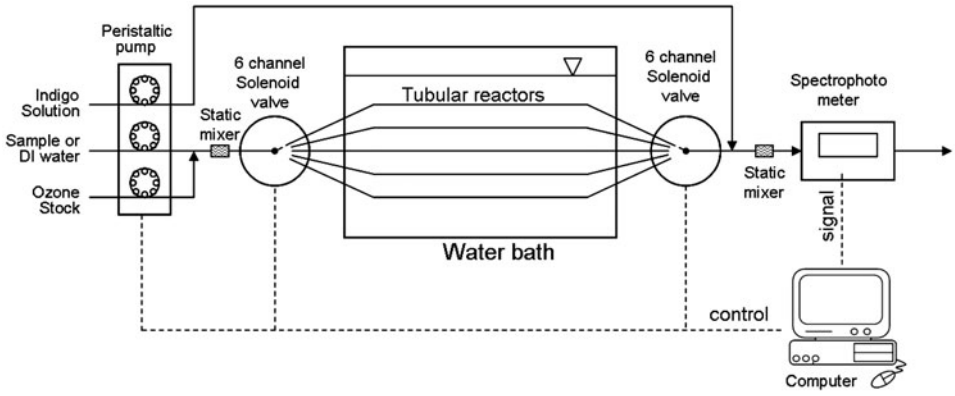

Fig. 2. A schematic diagram of the MC-SFR.

$$\frac{d[D]}{dt} = -k_R[D] \cdot [O_3] \quad (9)$$

where $[D]$ is the ozone demand and k_R the second-order rate constant for the decreased ozone demand.

The acquisition of the ozone decay kinetic parameters (i.e. k_R, k_D, and fast ozone demand $[D]_0$) from raw experimental data was challenging because three unknown parameters needed to be obtained using two first-order differential equations and a set of experimental data from the MC-SFR. Furthermore, optimizing kinetic parameters added further difficulty to data processing. $[D]_0$ and k_D were obtained by linear regression of $\ln([O_3])$ and time (t), where $[D]_0$ and k_D corresponded to "the difference between the initial ozone concentration and the y-intersect of the regression line" and "the slope," respectively. Obtaining k_R was more challenging than the other parameters. The method used was based on least-squaring the difference between the experimental and calculated ozone concentrations, which is explained in detail by Kim et al. [15].

Table 1 shows the experimental ozone decay of the sand-filtered water sample at three temperatures (i.e. 5, 15, and 25°C) and three pH values (i.e. 6.0, 7.0, and 8.0) with an initial ozone concentration of 1.5 mg/L [20]. The qualities of the water sample used throughout this study were TOC 1.4 mg/L, UV_{254} 0.02 (1/cm), pH 6.8, Br^- 9.5 μg/L, and turbidity 0.419 NTU. The bromate formation kinetics at three pH values and temperatures are summarized in Table 2 [20]. The formation kinetic coefficients are quite small because of low bromide concentration of the raw water. Note that bromide concentration was as low as 9.5 μg/L in the sample.

The tracer results, shown in Fig. 3, matched well with ADR model with a dispersion number (d) of 0.03. Thus, the ADR model could be applied to the full-scale ozone rector in order to study the effect of the dispersion number (d), ranging from 0.01 to 5.0, using nine ozone decay kinetic coefficients from sand-filtered raw water samples with three pH values and three temperatures. The initial ozone concentration was assumed to be 1.5 mg/L which is generally used for ozonation to inactivate *C. parvum* oocyst. Axial dispersion in an ozone contactor affects ozone concentration, log inactivation efficiency, and disinfection by-product formation [14,15,21,22]. Lower dispersion numbers are known to increase log inactivation efficiency [22,23] and thus could reduce bromate formation by reducing ozone dosing [14,24].

Table 1
Ozone decay kinetics of sand filtrate at three pHs and three temperatures

	pH 6.0			pH 7.0			pH 8.0		
Temp.(°C)	k_d (1/min)	$[D]_0$ (mg/L)	k_r (L/mg min)	k_d (1/min)	$[D]_0$ (mg/L)	k_r (L/mg min)	k_d (1/min)	$[D]_0$ (mg/L)	k_r (L/mg min)
5	0.024	0.16	0.971	0.038	0.10	1.918	0.047	0.17	1.439
15	0.034	0.24	1.501	0.065	0.38	2.139	0.073	0.59	1.915
25	0.054	0.48	2.238	0.112	0.68	2.572	0.152	0.84	9.000

Table 2
Bromate formation kinetic constants and amount of initial fast bromate formation for different pHs and different temperatures. unit: (μg BrO_3^-/L)/(min·mgO_3/L) for $k_BrO_3^-$

	pH 6.0		pH 7.0		pH 8.0	
Temp.(℃)	$k_BrO_3^-$	$[BrO_3^-]_0$ (μg/L)	$k_BrO_3^-$	$[BrO_3^-]_0$ (μg/L)	$k_BrO_3^-$	$[BrO_3^-]_0$ (μg/L)
5	0	1.94	0.066	1.58	0.080	1.76
15	0.008	1.68	0.099	1.42	0.111	1.73
25	0.025	1.65	0.100	1.38	0.110	1.87

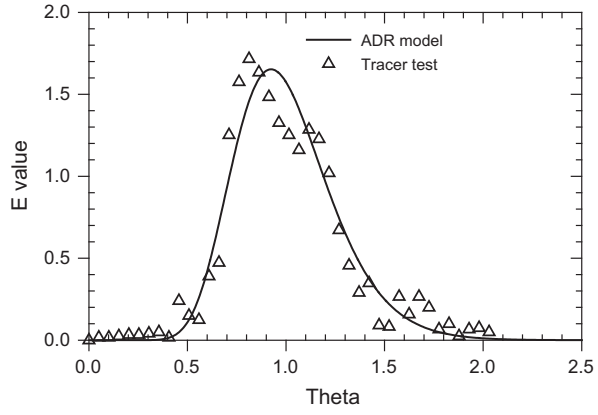

Fig. 3. Tracer test result of the full-scale ozone contactor (flow = 158,000 m^3/d) and fitting with ADR model.

The effect of the dispersion number on *C. parvum* oocyst log inactivation is shown in Fig. 4. Log inactivation is sensitively influenced by the dispersion number (*d*) when the dispersion number was relatively small and the inactivation rates were high (e.g. pH 6.0 and 7.0 at 25℃). The dispersion number 0.01 at pH 6.0 and 25℃ showed 34% higher log inactivation than the dispersion number 5.0 in the same condition. From this figure, it was interesting to note that reducing dispersion from 0.5 to 0.1 would be much more advantageous than reducing it from 5 to 0.5. In addition, inactivation of *Giardia lambria* and virus might be more sensitive to the dispersion number because it had much higher inactivation rate than *C. parvum* oocyst under the same CT conditions using ozone [25].

Residual ozone concentration was not affected much by decreased dispersion number as shown at Fig. 5. Residual ozone concentration became lower with smaller dispersion number, which was beneficial for the operation of ozone reactor since it should be removed at the outlet. As the ozone decay rate was increased (e.g. pH 8.0 and 25℃), the residual ozone concentration was more sensitively affected by dispersion number as shown in Fig. 5. On the contrary, residual ozone at low decay rate (e.g. pH 6.0 and 5℃) was less sensitively affected by dispersion number. Dispersion effect on CT (i.e. ozone concentration times, hydraulic contacting time) was shown in Fig. 6. CT differences between dispersion number 0.01 and 5.0 ranged from 3 to 5% for nine simulations. The influence of dispersion on CT was also minor as the residual ozone concentration. CT was highest at pH 6.0 and 5℃ in which condition residual ozone concentration was highest among nine simulation conditions.

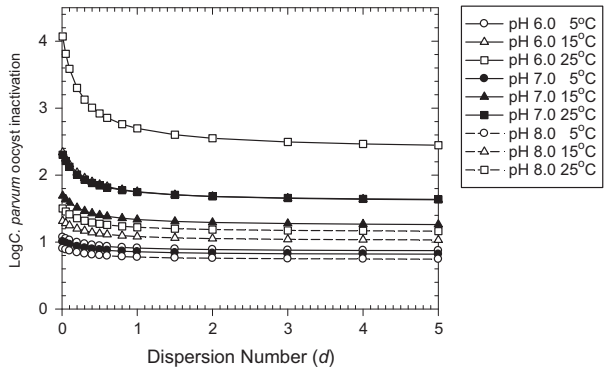

Fig. 4. *C. parvum* oocyst log inactivation as a function of dispersion number at different pHs and temperatures.

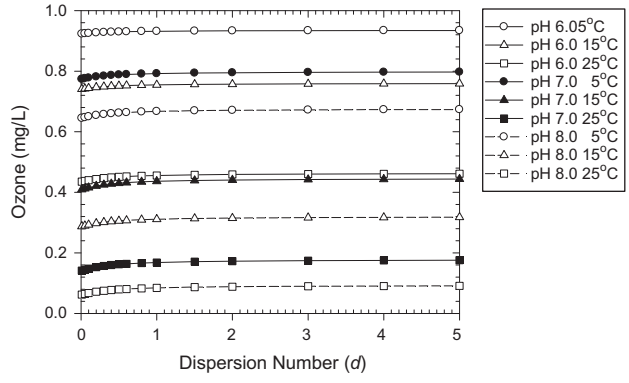

Fig. 5. Residual ozone as a function of dispersion number at different pHs and temperatures.

Bromate formation is influenced by both CT and the formation rate from bromide to bromate. Bromate formation was negligibly affected by the dispersion number as shown in Fig. 7. Although the bromate formation was highest at pH 6.0 and 5˚C, its difference between dispersion numbers 0.01 and 5.0 was only 2%. It was because its influence of the dispersion number on CT was minor and bromide concentration was very low in raw water. Hence, the advantage of enhanced *C. parvum* oocyst log inactivation at lower dispersion number region was not adversely affected by the boosted bromate formation.

Designing an ozone contactor with smaller dispersion number (especially less than 0.5) is beneficial for higher inactivation efficiency and saving ozone dosing. It was shown that the full- scale ozone contactor has a dispersion number of 0.03, which is extremely favorable for pathogen inactivation and saving ozone. For turbulent flow, axial diffusivity for single-phase flow could be expressed as Eq. (10) [26].

$$E = 0.25 \times D_p \times U \tag{10}$$

where E is the axial diffusivity (m^2/s), D_p is the pipe diameter (m), and U is the axial velocity (m/s). Eq. (11) could be obtained by combining Eqs. (10) and (1).

$$d = \frac{E}{UL} = \frac{0.25 \times D_p \times U}{UL} = \frac{0.25}{\left(\frac{L}{D_p}\right)} \tag{11}$$

The theoretical dispersion number of an ozone contactor in turbulent flow region could be obtained using Eq. (11). Since the ozone contactor shown in Fig. 1 had open channel hydraulics, the pipe diameter (D_p) could be replaced with the hydraulic diameter (D_H), defined as in Eq. (12).

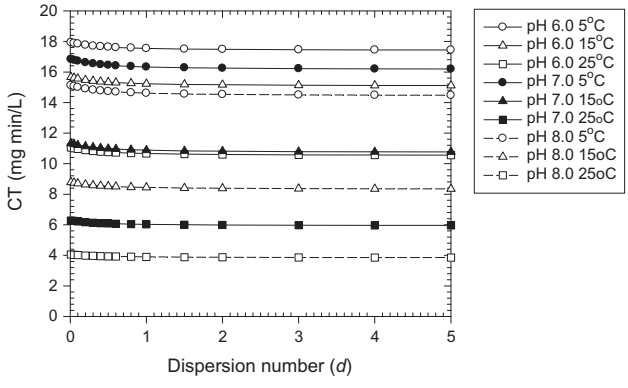

Fig. 6. CT as a function of dispersion number at different pHs and temperatures.

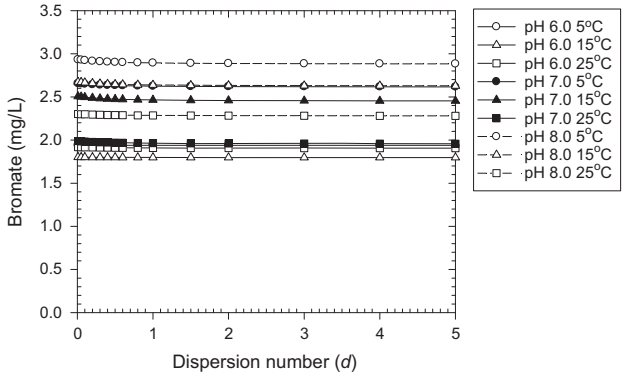

Fig. 7. Bromate formation as a function of dispersion number at different pHs and temperatures.

$$D_H = \frac{4 \times A}{P} \tag{12}$$

where A is the cross-sectional area (m^2) and P is the wetted perimeter (m). Eq. (12) shows that smaller hydraulic diameter and longer channel length were beneficial for lower dispersion number. The theoretical dispersion number of 0.013 was obtained for the full-scale ozone contactor with 4.6 m hydraulic diameter using Eq. (12), which was smaller than the observed dispersion number of 0.03 obtained from the full-scale tracer test. The difference might be caused by the meandering flow between chambers which may increase diffusivity at the turning point and by sudden change in hydraulic diameter at the first and last chambers. Thus, the ozone contactor might have more room to reduce dispersion number if the geometry of this contactor could be further optimized. For example, internal curved guiding baffles at the turning point of the channel might decrease the dispersion number [27].

The n-CSTRs in series model has been applied as another option to decrease dispersion number. Note that increasing the number of successive chambers could decrease dispersion number. The n-CSTRs in series could be implemented by multiple up-and down-vertical flow chambers in a full-scale ozone contactor. The dispersion number of an ozone contactor with multiple successive CSTRs in series could be acquired using Eq. (13), proposed by Villermaux [28]. The dispersion number of 0.03 could be obtained from 16 chambers in series using this equation. Since the observed dispersion number of the actual ozone contactor is generally larger than the theoretical one as the

results of non-ideal flow show (i.e. short-circuiting, back-flow, and stagnant zone) [27], more than 16 chambers would be necessary to obtain the dispersion number. That is, non-ideal flow in a multiple-chambered ozone reactor with vertical flow could increase the dispersion number and thus the number of chambers [29]. Furthermore, 16 CSTRs in series might be impractical considering increased capital cost and reduced ozone reactor volume by baffle wall. Hence, an ozone contactor with horizontal meandering flow seems to be beneficial for disinfection efficacy compared to a vertical flow one with multiple chambers in hydrodynamic characteristics.

$$\mathrm{Pe} = \frac{1}{d} = 2.0 \times N + 1 \tag{13}$$

where Pe is the Péclet number and N is the number of chambers.

4. Conclusions

The axial dispersion number 0.01 at pH 6.0 and 25˚C showed 34% higher inactivation efficiency than the dispersion number 5.0 for *C. parvum oocyst* from mathematical simulation using ADR model and ozone decay kinetics obtained from raw water. *C. parvum* oocyst inactivation was affected more sensitively by dispersion number when it was smaller than 0.5. On the contrary, the influences of dispersion number on the residual ozone, CT, and bromate formation were small. An equation was developed to calculate an axial dispersion number of a horizontal meandering flow ozone contactor using the length and wetted perimeter. The calculated dispersion number was smaller than the observed one. The reason is thought to be related to flow disturbance at the turning point between chamber and by sudden change in hydraulic diameter at the first and last chambers.

Acknowledgment

This research was supported by a grant (12-TI-C01) from Advanced Water Management Research Program funded by the Ministry of Land, Infrastructure and Transport of Korean government.

References

[1] L.L. Gyürék, H.B. Li, M. Belosevic, G.R. Finch, Ozone inactivation kinetics of *Cryptosporidium* in phosphate buffer, J. Environ. Eng. 125 (1999) 913–924.
[2] J.L. Rennecker, B.J. Mariñas, J.H. Owens, E.W. Rice, Inactivation of *Cryptosporidium parvum* oocysts with ozone, Water Res. 33 (1999) 2481–2488.
[3] J.L. Rennecker, A.M. Driedger, S.A. Rubin, B.J. Mariñas, Synergy in sequential inactivation of *Cryptosporidium parvum* with ozone/free chlorine and ozone/monochloramine, Water Res. 34 (2000) 4121–4130.
[4] D.A. Reckhow, B. Legube, P.C. Singer, The ozonation of organic halide precursors—Effect of bicarbonate, Water Res. 20 (1986) 987–998.
[5] J. Hoigné, H. Bader, The formation of trichloronitromethane (chloropicrin) and chloroform in a combined ozonation/chlorination treatment of drinking water, Water Res. 22 (1988) 313–319.
[6] J. Dojlido, E. Zbieć, R. Świetlik, Formation of the haloacetic acids during ozonation and chlorination of water in Warsaw waterworks (Poland), Water Res. 33 (1999) 3111–3118.
[7] G.R. Finch, M. Belosevic, Controlling *Giardia* spp. and *Cryptosporidium* spp. in drinking water by microbial reduction processes, Can. J. Civ. Eng. 28 (2001) 67–80.
[8] WHO, IARC Monographs on the Evaluation of Carcinogenic Risks to Humans, WHO, Geneva, 1990.
[9] USEPA, Fed. Reg. 59(145) (1994) 33668.
[10] M. Siddiqui, W.Y. Zhai, G. Amy, C. Mysore, Bromate ion removal by activated carbon, Water Res. 30 (1996) 1651–1660.
[11] O. Levenspiel, Chemical Reaction Engineering, third ed., John Wiley & Sons, New York, NY, 1999.
[12] M. Roustan, C. Beck, O. Wable, J.P. Duguet, J. Mallevialle, Modeling hydraulics of ozone contactors, Ozone Sci. Eng. 15 (1993) 213–226.
[13] H.S. Kim, H. Yamada, H. Tsuno, Control of bromate ion and brominated organic compounds formation during ozone/hydrogen peroxide treatment of secondary effluent, Water Sci. Technol. 53 (2006) 169–174.
[14] M. Roustan, J.P. Duguet, J.M. Laine, Z. DoQuang, J. Mallevialle, Bromate ion formation: Impact of ozone contactor hydraulics and operating conditions, Ozone Sci. Eng. 18 (1996) 87–97.
[15] D. Kim, S. Hasan, G. Tang, B.J. Mariñas, L. Couillard, H. Shukairy, J.-H. Kim, Simultaneous simulation of pathogen inactivation and bromate formation in full scale ozone contactors, J. AWWA 99 (2006) 77–91.
[16] G. Tang, K. Adu-Sarkodie, D. Kim, J.H. Kim, S. Teefy, H.M. Shukairy, B.J. Mariñas, Modeling *Cryptosporidium parvum* oocyst inactivation and bromate formation in a full-scale ozone contactor, Environ. Sci. Technol. 39 (2005) 9343–9350.
[17] D. Kim, J.D. Fortner, J.-H. Kim, A multi-channel stopped-flow reactor for measuring ozone decay rate: Instrument development and application, Ozone Sci. Eng. 29 (2006) 121–129.
[18] P.C. Singer, C.S. Hull, Modeling Dissolved Ozone Behavior in Ozone Contactors, AWWA Research Foundation, Denver, CO, 2000.
[19] O. Lev, S. Regli, Evaluation of Ozone Disinfection Systems—Characteristic Concentration C, J. Environ. Eng. 118 (1992) 477–494.
[20] D. Kim, J. Cho, Obtaining real-time kinetic parameters on ozone decay from a full-scale ozone contactor using the axial dispersion reactor model, Ozone Sci. Eng. 36 (2014) 100–109.

[21] Z. Do-Quang, C.C. Ramirez, M. Roustan, Influence of geometrical characteristics and operating conditions on the effectiveness of ozone contacting in fine-bubbles conventional diffusion reactors, Ozone Sci. Eng. 22 (2000) 369–378.
[22] J.H. Kim, U. von Gunten, B.J. Mariñas, Simultaneous prediction of *Cryptosporidium parvum* oocyst inactivation and bromate formation during ozonation of synthetic waters, Environ. Sci. Technol. 38 (2004) 2232–2241.
[23] Z. Do-Quang, M. Roustan, J.P. Duguet, Mathematical modeling of theoretical *Cryptosporidium* inactivation in full-scale ozonation reactors, Ozone Sci. Eng. 22 (2000) 99–111.
[24] J.H. Kim, M.S. Elovitz, U. von Gunten, H.M. Shukairy, B.J. Mariñas, Modeling *Cryptosporidium parvum* oocyst inactivation and bromate in a flow-through ozone contactor treating natural water, Water Res. 41 (2007) 467–475.
[25] K.L. Rakness, I. Najm, M. Elovitz, D. Rexing, S. via, *Cryptosporidium* log-inactivation with ozone using effluent CT10, geometric mean CT10, extended integrated CT10 and extended CSTR calculations, Ozone Sci. Eng. 27 (2005) 335–350.
[26] S. Moustiri, G. Hebrard, S. Thakre, M. Roustan, A unified correlation for predicting liquid axial dispersion coefficient in bubble columns, Chem. Eng. Sci. 56 (2001) 1041–1047.
[27] D. Kim, M. Elovitz, P.J.W. Roberts, J. Kim, Using 3D LIF to investigate and improve performance of a multichamber ozone contactor, J. AWWA 102 (2010) 61–70.
[28] J. Villermaux, Chemical Reaction Engineering, Second ed., Editions and Tec Doc / Lavoisier, Paris, 1993.
[29] D. Kim, T. Stoesser, J.H. Kim, The effect of baffle spacing on hydrodynamics and solute transport in serpentine contact tanks, J. Hydraul. Res. 51 (2013) 558–568.